21^{st} *Computer Vision Winter Workshop*
Luka Čehovin, Rok Mandeljc, Vitomir Štruc (eds.)
Rimske Toplice, Slovenia, February 3–5, 2016

Touching without vision: terrain perception in sensory deprived environments

Vojtěch Šalanský*, Vladimír Kubelka*†, Karel Zimmermann*, Michal Reinstein*, Tomáš Svoboda*†

Abstract. *In this paper we demonstrate a combined hardware and software solution that enhances sensor suite and perception capabilities of a mobile robot intended for real Urban Search & Rescue missions. A common fail-case, when exploring unknown environment of a disaster site, is the outage or deterioration of exteroceptive sensory measurements that the robot heavily relies on—especially for localization and navigation purposes. Deprivation of visual and laser modalities caused by dense smoke motivated us to develop a novel solution comprised of force sensor arrays embedded into tracks of our platform. Furthermore, we also exploit a robotic arm for active perception in cases when the prediction based on force sensors is too uncertain. Beside the integration of hardware, we also propose a framework exploiting Gaussian processes followed by Gibb's sampling to process raw sensor measurements and provide probabilistic interpretation of the underlying terrain profile. In the final, the profile is perceived by proprioceptive means only and successfully substitutes for the lack of exteroceptive measurements in the close vicinity of the robot, when traversing unknown and unseen obstacles. We evaluated our solution on real world terrains.*

1. Introduction

Advances in robotic technology allow mobile robots to be deployed in gradually more and more challenging environments. However, real-world conditions often complicate or even prohibit adoption of classical approaches to localization, mapping, navigation, or teleoperation. When rescuers operate a UGV during joint experiments in the TRADR project[1], which develops novel software and technology for human-robot teams in disaster response efforts [1], we have to deal with such problems.

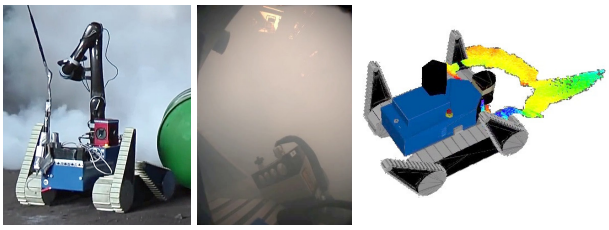

Figure 1. From left: UGV robot approaches smoke area; Example of visual information that the operator sees inside a cloud of smoke: a crop out from the omnidirectional camera (middle) and output of the laser rangefinder (rainbow-colored point cloud in the right half of the image). Laser beams are randomly reflected by smoke particles. The resulting 3D point cloud is just noise close to the robot.

One of the crucial fail-cases is the presence of dense smoke that blocks camera view and spoils laser measurements, creating false obstacles in front of the robot (Fig. 1). Without exteroceptive measurements, classical approaches to robot SLAM cannot be used. Localization can only be in the dead-reckoning sense and the operator of the robot has to rely solely on the maps created up to the point of the sensor outage. In an industrial environment consisting of many hazardous areas, driving blind can lead to damage or loss of the robot.

Therefore, we propose a combined hardware and software solution to predict the profile of terrain underneath and in front of the tracked robot. The algorithm exploits a prototype of a force sensor array installed inside a track of the robot, a robotic arm attached to the robot, proprioceptive measurements from joints and an inertial measurement unit (IMU), and information learned from a dataset of traversed terrains. The prototype of the force sensor (Fig. 2, 3) is suitable for tracked robots and is installed between rubber track and its support, allowing it to serve as

*Authors are with the Faculty of Electrical Engineering, Czech Technical University in Prague, {salanvoj, kubelvla, reinstein.michal, zimmerk, svobodat}@fel.cvut.cz

†Authors are with the Czech Institute of Informatics, Robotics and Cybernetics, Czech Technical University in Prague

[1] http://www.tradr-project.eu

a tactile sensor. The arm is used to measure height of terrain outside the reach of the force sensor as contact between the arm end-effector and the terrain. The height of terrain that cannot be measured directly is estimated by sampling from a joint probability distribution of terrain heights, conditioned by proprioceptive measurements (geometric configuration of the robot, torques in joints and attitude of the robot) and learned from a training dataset consisting of real-world examples of traversed terrains.

The estimates of terrain profile are used as a partial substitute for missing laser range-finder data that would reveal obstacles or serve as an input for adaptive traversability algorithm.

Our contribution is twofold: we designed a new force sensor suitable for tracked robots as well as an algorithm that uses proprioceptive and tactile measurements to estimate terrain shape in conditions that prohibit usage of cameras and laser range-finders. We extended this solution with robotic arm to deal with special cases when the predictions have too high uncertainty.

The rest of the paper is structured as follows: Section II concludes briefly the related work, Section III describes the hardware solution and Section IV the actual software. In Section V we present both qualitative and quantitative experimental evaluation and we conclude our achievements in Section VI.

2. Related work

The problem of terrain characterization primarily using proprioceptive sensors, but also by sonar/infrared range-finders and by a microphone is discussed in [2]. The authors exploit neural networks trained for each sensor and demonstrate that they are able to recognize different categories: gravel, grass, sand, pavement and dirt surface. More recent results come from legged robotics, in [3], Pitman-Yor process mixture of Gaussians is used to learn terrain types both in supervised and unsupervised manner based on force and torque features sensed in legs. In our work, we focus more on the actual terrain profile prediction, necessary for successful traversal.

Lack of sufficient visual information related to danger of collision with obstacles is addressed in [4]: decision whether it is safe to navigate through vegetation is based on wide-band radar measurements since it is impossible to detect solid obstacle behind vegetation from laser range-finder or visual data. Artificial whiskers offer an alternative solution; they mimic facial whiskers of animals and using them as a tactile sensor is a promising way to explore areas, which are prohibitive to standard exteroceptive sensors. Work of [5] presents a way to use array of actively actuated whiskers to discriminate various surface textures. In [6], similar sensor is used for a SLAM task. Two sensing modalities—the whisker sensor array and the wheel odometry are used to build a 2D occupancy map. Robot localization is then performed using particle filter with particles representing one second long "whisk periods". During these periods, the sensor actively builds local model of the obstacle it touches. Unfortunately, design of our platform does not allow using such whiskers due to rotating laser range-finder.

Relation between shape of terrain that we are interested in and configuration of the flippers is investigated in [7]. The authors exploit the knowledge about robot configuration and torques in joints to define a set of rules for climbing and descending obstacles not observed by exteroceptive sensors. We investigated this problem in [8] by introducing the adaptive traversability algorithm based on machine learning. We collected features from both proprioceptive and exteroceptive sensors to learn a policy that ensures safe traversal over obstacles by adjusting robot morphology. An idea of adding pressure sensors mimicking properties of human skin to feet of bipedal robots is presented in [9, 10]. These sensors can be used for measuring force distribution between the robotic foot and ground, or for terrain type classification. In tracked robots, caterpillar tracks can be further used to explore terrain, authors of [11] propose a novel distributed sensor that detects deflection of the track in contact points with terrain. Their sensor is especially suitable for chained tracks with rubber shoes. The prototype we present is more suitable for thin rubber tracks.

On contrary to the approaches exploiting only simple contact sensors, we extend our sensory suite with a robotic arm for further active perception for cases if necessary. Related to the active perception, relevant ideas and techniques come from the field of haptics. The work of [12] proposes to create models of objects in order to be able to grasp them. The idea is to complement visual measurements by tactile ones by strategically touching the object in areas with high shape uncertainty. For this purpose they use Gaussian processes (GP, [13]) to express the shape of the object. We take a similar approach: we

choose parts of terrain to be explored by the robotic arm based on uncertainty of the estimate resulting from the sampling process (Sec. 4.3). Probabilistic approach to express uncertainty in touched points is also described in [14], where only tactile sensors of a robotic hand are used to reconstruct the shape of an unknown object. Active tactile terrain exploration can also lead to terrain type classification, as works of [15, 16] demonstrate.

3. Sensors

3.1. Sensors of the TRADR UGV

The *TRADR* UGV platform is equipped with both proprioceptive and exteroceptive sensors. Inertial measurement unit *Xsens MTi-G* (IMU) provides basic attitude measurements; all joints have angle encoders installed to reveal current configuration of the robot like flipper angles, and velocity of the caterpillar tracks. Electric currents to all motors are measured and translated into torque values. Visual information about the environment is acquired by an omni-directional *Point Grey Ladybug 3* camera accompanied by a rotating *SICK LMS-151* laser range finder that provides depth information. The laser range-finder is used to collect data that are processed to serve as ground truth for the terrain reconstruction purposes.

3.2. Prototype of force sensor

To obtain well-defined contact points with the ground, we decided to take advantage of the flippers that can reach in front of the robot and are designed to operate on dirty surfaces or sharp edges. The original mechatronics of the robot allows to measure torque in flipper servos and thus detect physical contact between flippers and the environment. To be able to locate the contact point on the flipper exactly, we designed a thin force sensor between the rubber track and its plastic support (see Fig. 2, 3). Since it is a first prototype, we use it only in one flipper and consider only symmetrical obstacles or steps. The sensor construction is a sandwich of two thin stripes of steel with *FSR 402* sensing elements between them which allows the rubber track to slide over it while measuring forces applied onto the track. There are six force sensing elements; the protecting sheet of steel distributes the force among them, the sensor is thus sensitive along its whole length.

The *FSR 402* sensing elements are passive sensors that exhibit decrease in resistance with increasing force; the force sensitivity range is $0.1 - 10\,\mathrm{N}$. To measure the resistance, we connect them in series with a fixed reference resistor forming a voltage divider. We apply 5 V to this divider and measure voltage on the reference resistor. We use an analog-to-digital converter expansion board for the Raspberry Pi computer to read the six voltages. We calibrate the voltage values for initial bias caused by the sandwich construction.

Figure 4 shows three examples of the sensor readings. The first case consists of a flipper touching flat floor. Although one would expect to see more or less equal distribution of the contact force along the flipper track, the torque generated by the flipper actually lifts the robot slightly and thus, most of the force con-

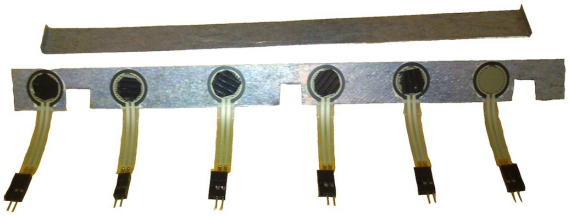

Figure 2. Prototype of the flipper force sensor: array of six sensing elements (FSR 402) is covered by a stripe of steel, forming a thin sensor that fits between the rubber track and the plastic track support. The stripe of steel protects the sensors from the moving rubber track and distributes measured force amongst them.

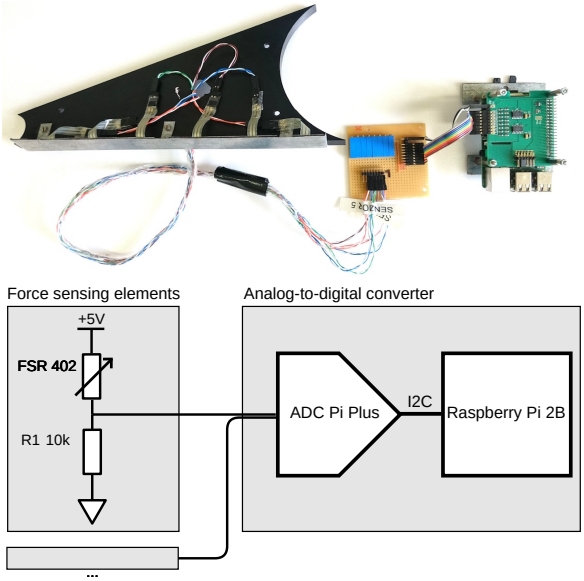

Figure 3. The sensor mounted to the plastic track support (top). The sensing elements are passive sensors that exhibit decrease in resistance with applied force. For each sensing element, we use a reference resistor to form a voltage divider; we obtain voltage inversely proportional to the resistance of the FSR 402 elements (bottom).

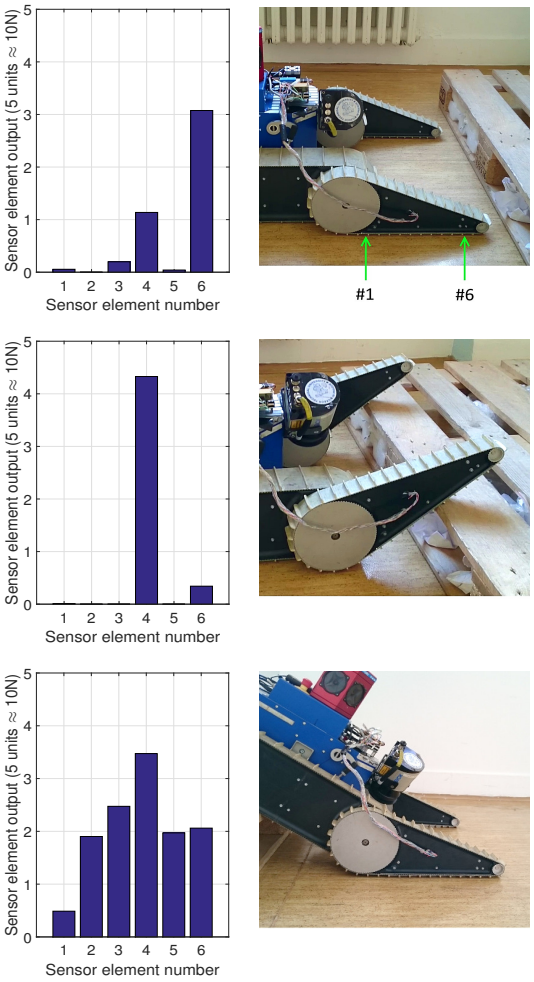

Figure 4. Examples of the force sensor readings. The plots on the left side show raw readings of each sensing element, only corrected for bias. The photos on the right side document the moments of the readings acquisition. See section 3 for discussion over the three example cases.

centrates at its tip (element n. 6). Compare this case with the third one (bottom), where the pose of the robot prohibits the lifting effect, and we therefore see the expected result. The second case (middle) shows an example of a touch in one isolated point.

3.3. Robotic arm

The UGV is equipped with a *Kinova Jaco* robotic arm[1], see Fig. 1 left. It is a 6-DOF manipulator (with one extra DOF in each finger) capable of lifting 1.5 kg. For our approach, it is used for tactile exploration of surroundings up to cca. 50 cm around the robot. For the terrain sensing, robotic arm holds a tool with a wooden stick—this setup protects its fingers from being broken when pushing against ground. It also allows the robot to measure the height of terrain in a chosen point by gradually lowering the arm until upsurge of actuator currents indicates contact with ground (there are currently no touch sensors) [17]. Accuracy of the measurement is 3 cm (standard deviation). However, the process of unfolding the arm, planning and execution of the desired motion and finally folding back to home position can easily take 45 s. Therefore, it is practical to use the arm for this purpose only in situations when the gain from the additional information overweights the cost of time spent to get it. In Section 4.4, we describe criterion for decision to use the arm.

[1] http://www.kinovarobotics.com/service-robotics/products/robot-arms

4. Terrain shape reconstruction

When robot is teleoperated operator's awareness is based on camera images and the 3D laser map. In the presence of smoke, both of these modalities are useless, see output of the operator console in the presence of smoke shown in Figure 1. We propose active tactile exploration mode (ATEM), in which flippers and robotic arm autonomously explores the terrain shape in close vicinity of the robot. Estimated terrain shape and expected reconstruction accuracy are eventually displayed to the operator.

If ATEM is requested by the operator, robot first adjusts flippers to press against the terrain and capture proprioceptive measurements. Then the initial probabilistic reconstruction of the underlying terrain shape is estimated from the captured data. If the reconstruction is ambiguous, the robotic arm explores the terrain height in the most inaccurate place. Eventually, the probabilistic reconstruction is repeated. As a result, reconstructed terrain shape with estimated variances is provided. The ATEM procedure is summarized in Algorithm 1. The rest of this section provides detailed description of particular steps.

4.1. Flipper exploration mode

As soon as the ATEM is requested, the robot halts driving and adjusts angles of front flippers towards ground until they reach an obstacle or the ground. They keep pressing against it by defined torque while vector of proprioceptive measurements $\mathbf{s}$ is captured. We measure: i) pitch of the robot (estimated from IMU sensor), ii) angles of flippers, iii) currents in flipper engines, and iv) 6-dimensional output of the force sensor.

Variables: $\mathbf{h}$ - vector of terrain bin heights,
$\mathbf{v}$ - vector of height variances,
$\mathbf{s}$ - vector of proprioceptive measurements.
while *ATEM is requested* **do**
  stop_robot;
  `// Invoke flipper exploration mode`
  `// Section 4.1`
  while torque_in_front_flippers $<$ threshold **do**
    push_flippers_down;
  end
  $\mathbf{s}$ = capture_proprioceptive_measurements();
  `// Perform kinematic reconstruction`
  `// Section 4.2`
  $[\mathbf{h}, \mathbf{v}]$ = kinematic_reconstruction($\mathbf{s}$);
  `// Perform probabilistic reconstr.`
  `// Section 4.3`
  $[\mathbf{h}, \mathbf{v}]$ = probabilistic_reconstruction($\mathbf{h}, \mathbf{v}, \mathbf{s}$);
  `// Invoke arm exploration`
  `// Section 4.4`
  if any($\mathbf{v} >$ threshold) **then**
    $[\mathbf{h}, \mathbf{v}]$ = arm_exploration($\mathbf{h}, \mathbf{v}$);
    $[\mathbf{h}, \mathbf{v}]$ = probabilistic_reconstruction($\mathbf{h}, \mathbf{v}, \mathbf{s}$);
  end
  move_forward;
end

Algorithm 1: Active tactile exploration mode for terrain shape reconstruction.

4.2. Kinematic reconstruction

The terrain shape is modeled by Digital Elevation Map (DEM), which consists of eleven 0.1 m-wide bins. If there is only one isolated contact point sensed by the force sensor and the force surpasses experimentally identified threshold (see Fig. 4, second case), the height $\mathbf{h}_i$ of the terrain in the corresponding bin i is estimated by a geometric construction from known robot kinematics, using the attitude of the robot, configuration of joints and the position of the contact point on the flipper. Variance $\mathbf{v}_i$ for the corresponding force sensor is set to an experimentally estimated value. The remaining $\mathbf{h}_i$ and $\mathbf{v}_i$ values are set to non-numbers.

4.3. Probabilistic reconstruction

In the probabilistic reconstruction procedure, the vector of heights $\mathbf{h}$ and the vector of variances $\mathbf{v}$ are estimated by the Gibbs sampling [18]. Let us denote the set of all bins J and the set of all bins in which the reconstruction is needed by I (i.e. those which height was not estimated in the kinematic reconstruction procedure or measured by the robotic arm). We use the Gibbs sampling to obtain height samples $\mathbf{h}_I^k$, $k = 1 \dots K$ from the joint probability distributions $p(\mathbf{h}_I | \mathbf{h}_{J \setminus I}, \boldsymbol{s})$ of all missing heights $\mathbf{h}_I$. Missing heights $\mathbf{h}_I$ are reconstructed as the mean of generated samples, variances $\mathbf{v}_I$ are estimated as the variance of samples.

In the beginning, the missing heights $\mathbf{h}_I$ are randomly initialized. The k-th sample $\mathbf{h}_I^k$ is obtained by iterating over all unknown bins $i \in I$ and generating their heights $\mathbf{h}_i^k$ from conditional probabilities $p(\mathbf{h}_i | \mathbf{h}_{J \setminus i}, \mathbf{s})$. The conditional probability is modeled by Gaussian process [19, 13, 20] with a squared exponential kernel.

To train the conditional probabilities, we collected real-world trajectories with i) sensor measurements $\mathbf{s}^u$ and ii) corresponding terrain shapes $\mathbf{h}^u$ estimated from the 3D laser map for $u = 1 \dots U$. The i-th conditional probability $p(\mathbf{h}_i | \mathbf{h}_{J \setminus i}, \mathbf{s})$ is modeled by one Gaussian process learned from the training set $\{[(\mathbf{h}_{J \setminus i}^1, \mathbf{s}^1)^\top, \mathbf{h}_i^1], \dots, [(\mathbf{h}_{J \setminus i}^U, \mathbf{s}^U)^\top, \mathbf{h}_i^U]\}$.

Modeling the bin height probabilities as normal distributions is a requirement laid by the Gaussian process. However, it allows samples of the bin height that collide with the body of robot, which is of course physically impossible. We propose to use Gaussian distribution truncated by known kinematic constraints, in which are samples constrained by the maximal height that does not collide with the body of the robot. We discuss impact of this modification in the Section 5.

4.4. Active arm exploration

We use the robotic arm to measure the height of the terrain in bins the flippers cannot reach. The measurement taken by the robotic arm is reasonably accurate and precise but in its current state it takes about 45s to complete [17]. If the probabilistic reconstruction contains bins with variance $\mathbf{v}$ higher than a user-defined threshold, the robotic arm is used to measure the height in the most uncertain bin, i.e. the bin $j = \arg\max_i \mathbf{v}_i$. The height sensed in the given bin is then fixed and the probabilistic reconstruction process is repeated.

5. Experimental evaluation

In qualitative experiments, we focus on typical cases of terrain profile shapes and discuss performance of different settings of our algorithm. In quantitative experiments, we present performance statistics over the whole testing dataset.

The *training dataset* consists of 28 runs containing driving on flat terrain, approaching obstacles of

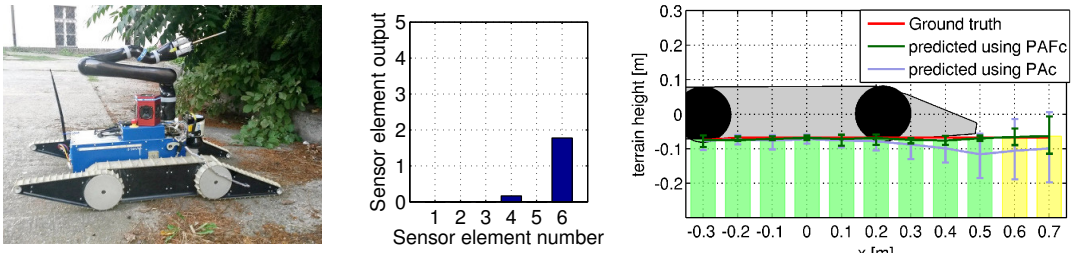

Figure 5. From left: photo of the robot on a concrete ground; measured forces; terrain reconstruction, the gray polygon indicates position of the robot and its flippers, thin red line is the ground truth—flat ground in this instance.

two different heights, traversing them and descending from them back to flat ground. Shape of obstacles selected for the dataset reflects the industrial accident scenario of the TRADR project - the environment mostly consists of right-angle-shaped concrete and steel objects. From the recorded runs, we have extracted approximately 1400 individual terrain profile measurements for training. The whole training dataset was recorded indoors on flat hard surfaces. The *testing dataset* was recorded outdoors and combines uneven grass, stone and rough concrete surfaces. It contains more complex obstacles with various heights (different from those seen in the training dataset). The testing dataset consists of more than 300 terrain profiles with the corresponding sensory data. Ground truth necessary for training and testing was created manually by sampling scans from the laser range-finder recorded during the experiments.

We compare four different algorithms for terrain profile prediction. The baseline approach [8] uses only the IMU sensor and angles of flippers, we call it PA (pitch + angle of flippers) for short. The second setup uses the same data and adds the probability of terrain height being adapted in the way described in Section 4.3. If the sampled height collides with the robot, the sample is set to the maximal possible height that is not in collision. The approach is called PAc (pitch + angle of flippers; constrained). The third approach adds the flipper force sensor; measured data are used in two ways. If the force measured by a sensor element exceeds a threshold (experimentally set on 2 units), then the height of the bin is computed from kinematics of the robot (pitch and flipper angles and position of the sensor element) and the bin is fixed and excluded from the Gibbs sampling step. It should be noted however, that the measured forces are used even if they are not bigger than the threshold – they are part of the proprioceptive data s. The approach is called as PAFc (pitch + angle of flippers + flipper force sensor; constrained). The fourth approach adds direct terrain measurement: we simulate use of the robotic arm for measurements the terrain height in bins with high uncertainty [17]. The simulation means revealing the value of the bin captured in the ground truth, variance of the bin is then equal to the variance of the arm measurements. In the experiments shown in this paper we set the standard deviation threshold of Gibbs samples that leads to arm exploration to 0.06 m. The fourth approach is called as PAFAc (pitch + angle of flippers + flipper force sensor + robotic arm; constrained).

5.1. Qualitative Evaluation

In the figures 5, 6 and 7, we present typical terrain profiles and robot actions: flat ground, two steps with different height, climbing up a step and stepping down of a step. We compare performance of two algorithms: i) PAc uses the kinematic constraints when sampling but does not use the force sensors (light blue line in the plots) ii) PAFc algorithm which uses the force sensors (green line and bars). The last two bars marked yellow in order to emphasize the predictions are learnt from training dataset and we do not have enough information to correct the predictions from the sensing by flippers.

We use mean of the (Gibbs) samples as the predicted value (connected by lines) and 0.1 and 0.9 quantiles for displaying dispersion of samples (errorbars). The point $(0, 0)$ coincides with the location of the IMU sensor inside the robot body. The depicted sketch of the robot: the pitch is estimated by IMU, flipper angle is directly measured. When the robot lies on a flat ground, Fig. 5, contact point is sensed by the sixth element. The force measurement reduces uncertainty mainly in positions $0.3 - 0.7$ m.

Climbing up a step cases are depicted in Fig. 6. The higher 0.28 m step obstacle is on top. The fifth sensor element measures the force that is bigger than threshold and the height in the bin 0.4 is fixed and not sampled. Note that algorithm PAc which does

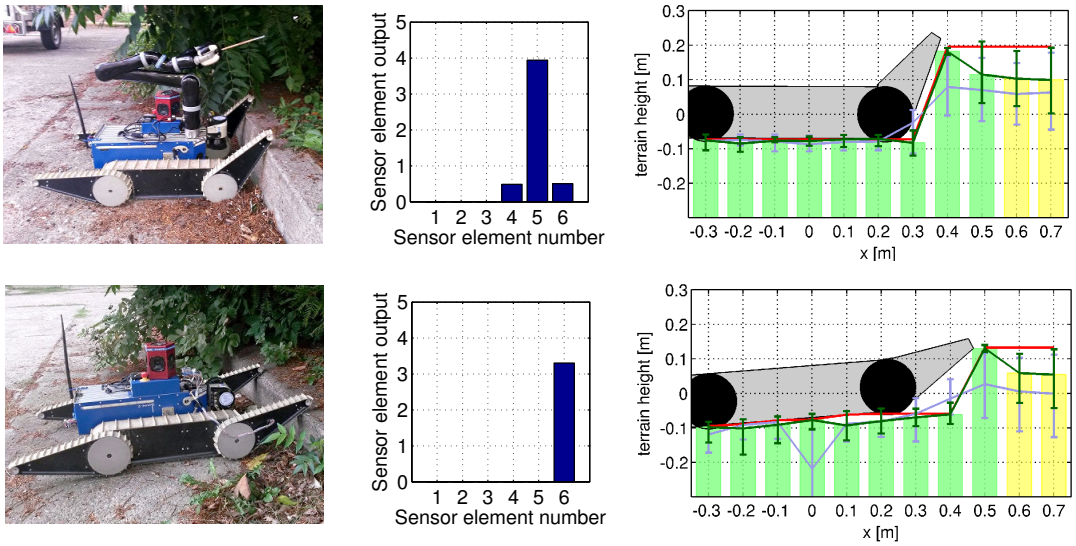

Figure 6. Top: 0.28 m step, bottom: 0.2 cm step. Note the reduced uncertainty for the PAFc – green line and errorbars. The top photo of the robot is flipped in order to preserve left-to-right orientation which should ease the visual comparison.

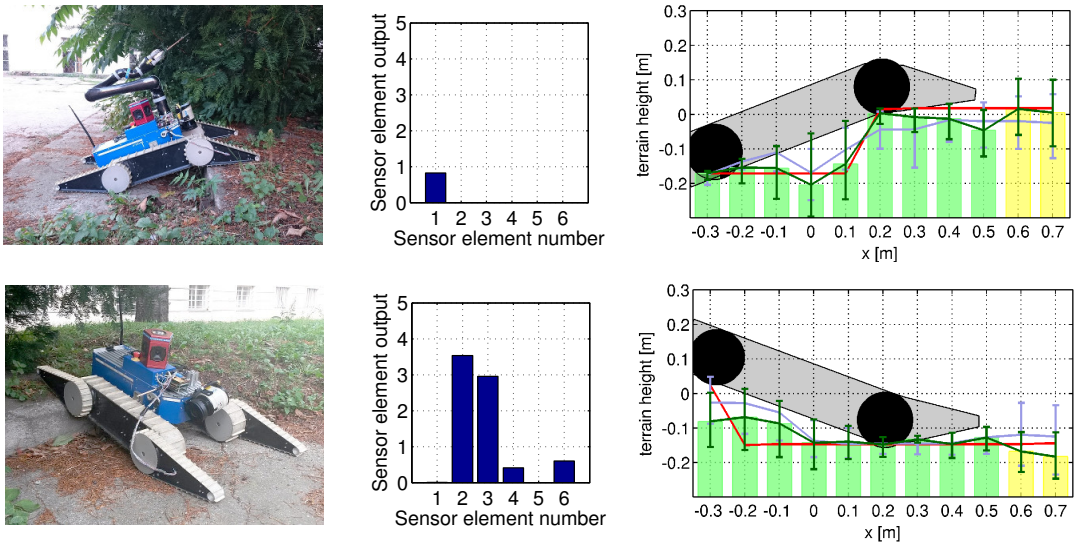

Figure 7. Top: climbing up a step; Bottom: stepping down of a step. When stepping down, the robot "hangs" on the rear flippers, not the main flippers.

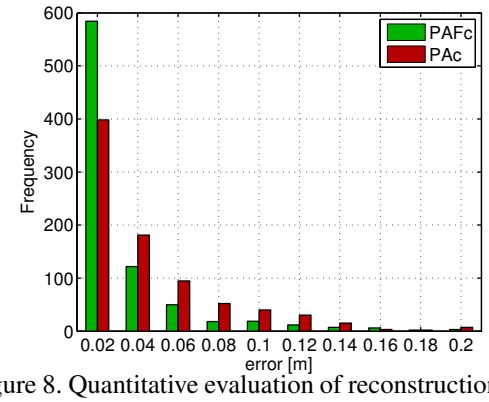

Figure 8. Quantitative evaluation of reconstruction quality in the places/bins that are under the flipper.

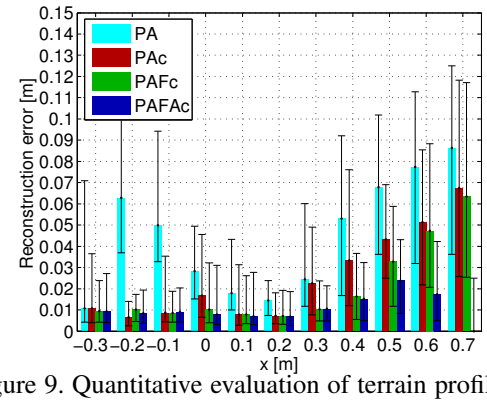

Figure 9. Quantitative evaluation of terrain profile reconstruction – for all the DEM bins. Median, 1st quartile and 3rd quartile of errors are shown

not use force sensor cannot predict the exact edge location. This fact is indicated by big dispersion of samples in bins 0.3 and 0.4. The second situation shown in Fig. 6 is the lower step. The height of the lower step 0.2 m was correctly measured by the sixth element of the force sensor.

Climbing up and stepping down cases are displayed in Fig. 7. Variances in the bins that are underneath the robot are high because we do not have enough information to estimate the correct heights. Still, the means are correct due to models learnt from the training data.

5.2. Quantitative Evaluation

As our metric of performance is the absolute error of estimated bin heights which is non-negative, we prefer to describe its statistical properties by quantile characteristics rather than by the means and standard deviations. The statistics are computed from the whole testing dataset - i.e. from more than 300 outdoor terrain profiles.

First, we measure the direct effect of the force measurement on the accuracy of the height estimates. The graph on Fig 8 shows the height error frequency of the DEM-bins that are underneath the front flipper. Note that the attribute "underneath the front flipper" is not fixed, it depends on the flipper angle. The force sensor indeed improves the accuracy over the using the flipper angle only.

The second experiment studies the statistics for all the DEM-bins individually, see Fig 9. Adding the kinematic contraint C naturally improves the estimates of the bins underneath the robot body $(-0.3 \ldots 0.2)$. Using the force sensors (PAFc) improves height estimates of the DEM-bins underneath the front flipper $(0.3 \ldots 0.5)$. The bins in front of the flippers, i.e. $(0.6$ and $0.7)$ are directly measurable only by the arm exploration. It is thus obvious that including the measurement by arm (PAFAc) has the dominant effect.

6. Conclusions

In this paper the aim was to demonstrate a combined hardware and software solution that enhances sensor suite and perception capabilities of our mobile robot intended for real Urban Search & Rescue missions. We focused our efforts on enabling proprioceptive terrain shape prediction for cases when vision and laser measurements are unavailable or deteriorated (such as in presence of a dense smoke). To evaluate our proposed solution experimentally, we designed and compared four algorithms—four possible approaches for proprioceptive terrain shape reconstruction: simple kinematics based approach, constrained kinematics, constrained kinematics with force sensors, and constrained kinematics with both force sensors and robotic arm—intended for special cases, where terrain prediction reaches very high uncertainty. From the presented qualitative and quantitative experimental evaluation we can clearly see that enhancing the sensor suite with force sensor array proves to be superior. The proposed algorithm, which combines Gaussian processes followed by Gibb's sampling, was successfully implemented on-board the robot to process the raw force measurements and perform the actual terrain shape prediction in a probabilistic manner. We certainly do not claim this is the only and best way to perform such terrain prediction, but, it definitely serves as sufficiently robust and accurate proof of concept for intended deployment. As part of this concept, the integration of robotic arm for active perception in cases when the prediction based on force sensors is too uncertain proved to be important. For future work, we aim to embed additional force sensor arrays on all the four robot flippers and extend the terrain prediction algorithm accordingly.

ACKNOWLEDGMENT

The authors were supported by the Czech Science Foundation GA14-13876S, the EU-FP7-ICT-609763 TRADR project and the Czech Technical University grant SGS15/081/OHK3/1T/13.

References

[1] I. Kruijff-Korbayová, F. Colas, M. Gianni, F. Pirri, J. de Greeff, K. V. Hindriks, M. A. Neerincx, P. Ögren, T. Svoboda, and R. Worst, "TRADR project: Long-term human-robot teaming for robot assisted disaster response," *KI*, vol. 29, no. 2, pp. 193–201, 2015. 1

[2] L. Ojeda, J. Borenstein, G. Witus, and R. Karlsen, "Terrain characterization and classification with a mobile robot," *Journal of Field Robotics*, vol. 23, no. 2, pp. 103–122, 2006. 2

[3] P. Dallaire, K. Walas, P. Giguere, and B. Chaibdraa, "Learning terrain types with the pitman-yor process mixtures of Gaussians for a legged robot," in *Intelligent Robots and Systems (IROS)*, 2015. 2

[4] J. Ahtiainen, T. Peynot, J. Saarinen, and S. Scheding, "Augmenting traversability maps with ultra-wideband radar to enhance obstacle detection in vegetated environments," in *Intelligent Robots and Systems (IROS)*, 2013. 2

[5] J. Sullivan, B. Mitchinson, M. Pearson, M. Evans, N. Lepora, C. Fox, C. Melhuish, and T. Prescott, "Tactile discrimination using active whisker sensors," *IEEE Sensors Journal*, vol. 12, no. 2, pp. 350–362, 2012. 2

[6] M. Pearson, C. Fox, J. Sullivan, T. Prescott, T. Pipe, and B. Mitchinson, "Simultaneous localisation and mapping on a multi-degree of freedom biomimetic whiskered robot," in *Robotics and Automation (ICRA)*, 2013. 2

[7] K. Ohno, S. Morimura, S. Tadokoro, E. Koyanagi, and T. Yoshida, "Semi-autonomous control system of rescue crawler robot having flippers for getting over unknown-steps," in *Intelligent Robots and Systems (IROS)*, 2007. 2

[8] K. Zimmermann, P. Zuzanek, M. Reinstein, T. Petricek, and V. Hlavac, "Adaptive traversability of partially occluded obstacles," in *Robotics and Automation (ICRA)*, 2015. 2, 6

[9] H. Lee, "Development of the robotic touch foot sensor for 2d walking robot, for studying rough terrain locomotion," Master's thesis, University of Kansas, June 2012, mechanical Engineering. 2

[10] J. Shill, E. Collins, E. Coyle, and J. Clark, "Terrain identification on a one-legged hopping robot using high-resolution pressure images," in *Robotics and Automation (ICRA)*, 2014. 2

[11] D. Inoue, M. Konyo, K. Ohno, and S. Tadokoro, "Contact points detection for tracked mobile robots using inclination of track chains," in *International Conference on Advanced Intelligent Mechatronics*, 2008, pp. 194–199. 2

[12] M. Bjorkman, Y. Bekiroglu, V. Hogman, and D. Kragic, "Enhancing visual perception of shape through tactile glances," in *Intelligent Robots and Systems (IROS)*, 2013. 2

[13] C. K. Williams and C. E. Rasmussen, "Gaussian processes for regression," in *Advances in Neural Information Processing Systems 8*, D. Touretzky, M. Mozer, and M. Hasselmo, Eds. The MIT Press, 1996, pp. 514–520. 3, 5

[14] M. Meier, M. Schöpfer, R. Haschke, and H. Ritter, "A probabilistic approach to tactile shape reconstruction," *Robotics, IEEE Transactions on*, vol. 27, no. 3, pp. 630–635, 2011. 3

[15] J. Romano and K. Kuchenbecker, "Methods for robotic tool-mediated haptic surface recognition," in *Haptics Symposium (HAPTICS), 2014 IEEE*, 2014, pp. 49–56. 3

[16] D. Xu, G. Loeb, and J. Fishel, "Tactile identification of objects using Bayesian exploration," in *Robotics and Automation (ICRA)*, 2013. 3

[17] V. Šalanský, "Contact terrain exploration for mobile robot," Master's thesis, Czech Technical University in Prague, 2015, in Czech. 4, 5, 6

[18] S. Geman and D. Geman, "Stochastic relaxation, gibbs distributions, and the bayesian restoration of images," *Pattern Analysis and Machine Intelligence, IEEE Transactions on*, no. 6, pp. 721–741, 1984. 5

[19] A. O'Hagan and J. Kingman, "Curve fitting and optimal design for prediction," *Journal of the Royal Statistical Society. Series B (Methodological)*, pp. 1–42, 1978. 5

[20] C. E. Rasmussen and H. Nickisch. Gpml matlab code. 5